REDUCING THE BAND-GAP ENERGY OF TiO_2 AS A CRUCIAL OBJECTIVE IN GREEN PHOTOCATALYSIS

Perica Paunović, Anita Grozdanov, Petre Makreski, Martin Stojčevski, Kiril Stoimčev, Gorazd Čepiševski

Faculty of Technology and Metallurgy, Ss. Cyril and Methodius University in Skopje, North Macedonia

pericap@tmf.ukim.edu.mk

Abstract: *Green photocatalysis focuses on developing processes to address various environmental challenges, such as the treatment of contaminated water and air, the generation of renewable energy, biomass management, carbon monoxide oxidation, and organic synthesis. TiO_2 nanoparticles are relatively inexpensive, non-toxic, and chemically stable. They are available in diverse structural forms and exhibit unique semiconductive properties, making them the most widely utilized photocatalysts in this domain. TiO_2 has a wide array of applications in green photocatalysis, including i) photocatalytic remediation and ii) the development of alternative, sustainable energy sources. A significant challenge in modern green photocatalysis is the reduction of the band gap energy (E_g), which is essential for determining the suitability of materials for photocatalytic activity. Decreasing E_g enables TiO_2 to effectively harness visible light rather than being limited to ultraviolet light. This study investigates the structural changes and subsequent reduction in E_g resulting from two types of TiO_2 modification: i) ionizing irradiation and ii) the incorporation of carbon nanotubes. We synthesized TiO2 nanoparticles using our proprietary sol-gel method, followed by thermal treatment at 400 °C. Structural changes were analyzed using X-ray powder diffraction (XRPD) and Raman spectroscopy, while the band gap energy of the samples was assessed through UV-Vis spectroscopy*.

Keywords: Green photocatalysis, TiO_2 nanoparticles, band-gap energy, ionizing irradiation, TiO_2/CNTs nanocomposites.

INTRODUCTION

Chemical processes driven by light and enhanced by suitable semiconductive materials, known as photocatalysts, are referred to as photocatalytic processes. These processes include three sequential steps as is shown in Fig.1 [1,2]. In the first step, when the photocatalytic material is exposed to light with energy that exceeds its band gap energy, electron-hole pairs are created. In the subsequent step, these electrons and holes move across the photocatalyst's surface and interact with surface water and oxygen, leading to the formation of radical species such as $^{\bullet}OH$ and $^{\bullet}O_2^-$. Finally, these generated radical species react with pollutant molecules, decomposing them into harmless substances like CO_2, H_2O, NO, NO_2, etc.

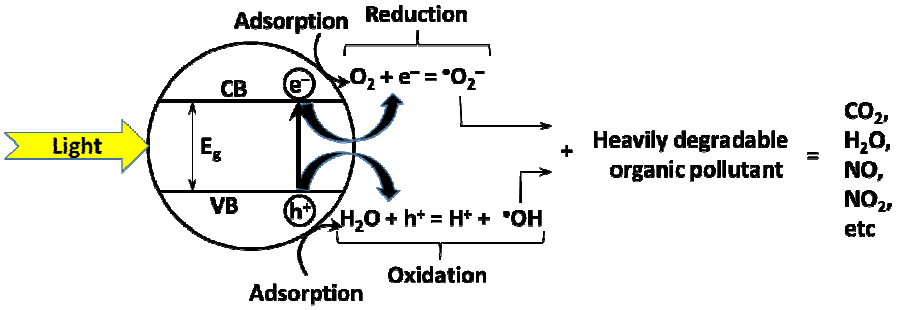

Figure 1 *Schematic view of the mechanism of the photocatalytic degradation of heavily degraded pollutant*

TiO_2 is renowned for its excellent semiconductive properties, making it an ideal photocatalyst and the most widely used material in photocatalysis. It is characterized by being low-cost, non-toxic, and chemically stable, and it is available in various polymorphic forms. In its nanoparticle form, TiO_2 demonstrates significantly enhanced photocatalytic activity compared to its bulk counterpart. The reduced particle size facilitates the easier movement of photoelectrons and holes to the surface, thereby lowering the recombination rate [3]. Additionally, nanostructured materials possess a greater surface-to-bulk atom ratio, which results in an increased real surface area and, subsequently, a significantly higher number of active photocatalytic centers.

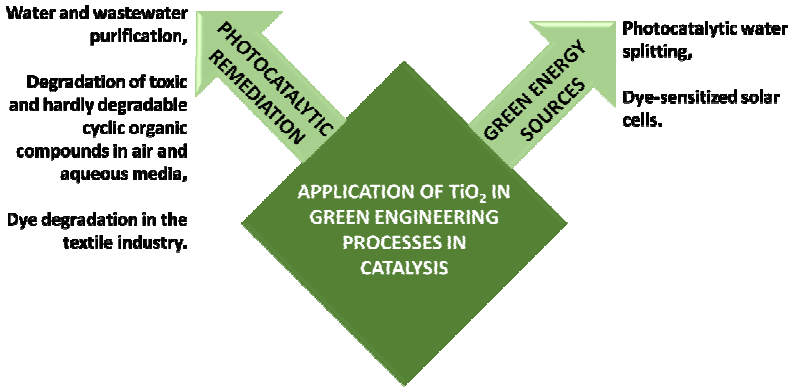

Figure 2 *The main application of TiO_2 in green photocatalysis*

In 1972, Fujishima and Honda [4] conducted groundbreaking research on photocatalytic water splitting utilizing a TiO_2 cathode, marking the dawn of a new era in photocatalysis. This landmark study spurred a notable increase in research focused on photocatalytic processes aimed at energy production and

environmental protection. As a photocatalyst, TiO_2 offers a wide variety of applications in green photocatalysis, including i) photocatalytic remediation and ii) alternative green energy sources, as illustrated in Fig. 2.

The band gap energy (E_g) is a key property that dictates the suitability of materials for photocatalytic applications. Additionally, the band gap is crucial for facilitating charge separation, which reduces recombination rates and enhances photocatalytic activity under specific wavelengths [3]. Titanium dioxide (TiO_2), classified as an n-type semiconductor, possesses a relatively wide energy band gap of 3.2 eV in its anatase form and 3.0 eV in its rutile form. Despite its larger energy band gap, anatase is regarded as a more effective photocatalyst [5], owing to its indirect band gap, as opposed to rutile's direct band gap. In the case of an indirect band gap, an excited electron can be stabilized at a lower level in the conduction band, leading to a prolonged lifespan and increased mobility. Moreover, due to its higher Fermi level compared to rutile, anatase demonstrates a stronger affinity for hydroxyl group ($^{\bullet}OH$) adsorption while exhibiting a lower affinity for oxygen adsorption.

A major limitation is that TiO_2 is most effective under ultraviolet (UV) light due to its wide band gap. It's worth noting that only approximately 4% of the solar spectrum is composed of UV light, resulting in a substantial amount of unused solar energy. As a result, a primary goal and challenge in photocatalysis is to develop photocatalysts that are active in visible light.

There are several techniques to reduce the band gap energy of TiO_2: 1) doping with various ions [6,7], 2) employing non-stoichiometric titanium oxides (Magneli phases) [8], 3) hydrogen plasma treatment [9], 4) exposure to ionizing radiation [10-12], and 5) compositing with CNTs [13,14].

This paper examines the structural changes in sol-gel prepared TiO_2 resulting from electron-beam and x-ray irradiation, as well as the effects of CNT compositing, and how these alterations influence the band gap energy.

EXPERIMENTAL

The TiO_2 nanoparticles the subject of study in this paper were prepared using the sol-gel method under normal atmospheric pressure. Titanium tetraisopropoxide (TTIP) at 97% purity from Aldrich was used as the precursor. The synthesis procedure is described elsewhere [15].

The as-prepared TiO_2 was subjected to two types of irradiation: electron-beam

irradiation (low energy and a corpuscular nature) and x-ray irradiation (high energy and a wave nature). Due to their significant differences in energy levels, the e-beam irradiation dose was set at 50 kGy, while the x-ray irradiation dose was only 7 mGy.

The TiO_2/CNTs nanocomposites were synthesized using a sol-gel method similar to that used for pure TiO_2. Before adding the TiO_2 precursor (TTIP), carbon nanotubes (CNTs) were adequately dispersed in absolute ethanol. Both single-walled carbon nanotubes (SWCNTs) and multi-walled carbon nanotubes (MWCNTs) were employed. The compositions of the nanocomposites examined were 80% TiO_2 + 20% MWCNTs and 80% TiO2 + 20% SWCNTs.

The structural analysis, which involved the identification of current structural phases and parameters, was conducted using X-ray powder diffraction (XRD) and Raman spectroscopy. A Rigaku Ultima IV diffractometer operating with CuKα radiation (λ = 1.54178 Å) was employed for XRD measurements. The X-ray tube voltage was set to 40 kV, with a current of 40 mA, and a Kβ filter was utilized. Diffraction patterns were recorded in the 20° to 80° range (2θ) at a rate of 5°/min using a D/teX Ultra high-speed (1D) detector. For micro-Raman spectrum collection, the Horiba Jobin Yvon LabRam 300 Infinity was utilized, using ANd:YAG frequency-doubled laser operating at 532 nm without an attenuation filter. The Raman peak of the silica wafer at 520.7 cm^{-1} facilitated the calibration of the Raman shift. A grating with 1800 grooves/mm was selected to disperse the signal onto the CCD detector, ensuring high dispersion and excellent spectral resolution.

The optical properties were studied using UV-Vis spectroscopy. The UV-Vis absorption spectra of the TiO_2-water suspension were collected with a Varian Cary Scan 50 spectrophotometer (Switzerland) in 1 cm quartz cells at a temperature of 25 °C, covering the range from 200 to 900 nm with a scan speed of 200 nm. These spectra were used to determine the energy of the band gap of the studied materials.

RESULTS AND DISCUSSIONS

According to the literature [16,17], exposure to ionizing radiation can cause structural changes in TiO_2, such as an increase in the Ti^{3+}/Ti^{4+} ratio and the creation of oxygen vacancies. These modifications may result in a decrease in band gap energy, thereby enhancing the photocatalytic activity under visible light. The interaction between CNTs and TiO_2 significantly extends the lifespan of electron-hole pairs. This improvement is due to the differing work functions of TiO_2 (4.2–4.3 eV [18]) and CNTs (4.7–5.1 eV [19]). Electrons migrate from the conduction

band of TiO2, which has a lower work function, to the CNTs, which have a higher work function. This transfer continues until the Fermi levels of both materials align, resulting in the formation of a Schottky barrier at their interface [20].

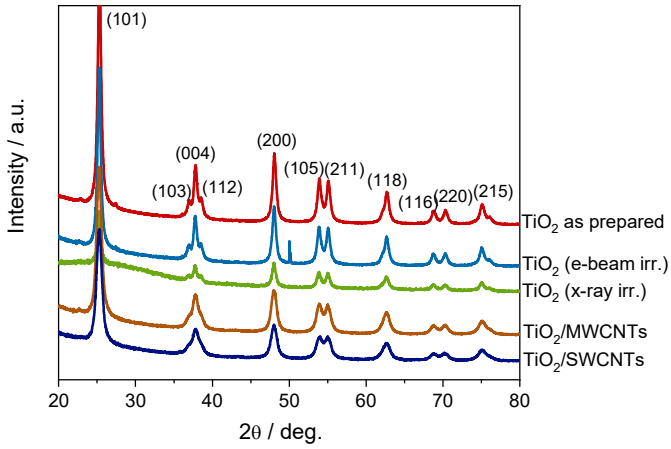

Figure 3 *XRD spectra of the studied TiO_2 samples*

Table 1 *Calculated values of interplanar distance, cell parameters, and particle size from XRD spectra and wave number values of the E_g Raman peaks*

Sample	$d_{\{101\}}$, Å	a, Å	c, Å	D, nm	E_g, cm^{-1}
as-prepared	3.5175	3.7832	9.5546	16.9	140.42
e-beam irradiated	3.5229	3.7860	9.6182	16.0	141.89
x-ray irradiated	3.5245	3.7874	9.6278	14.5	144.45
TiO_2/MWCNTs	3.5216	3.7872	9.5724	12.8	137.10
TiO_2/SWCNTs	3.5233	3.7888	9.5807	10.0	133.13

To identify the crystalline form of TiO_2 and assess the changes at the crystalline level, including crystal parameters and nanoparticle size, the samples were analyzed using X-ray diffraction (XRD). The XRD spectra presented in Figure 3 clearly display the characteristic features of the anatase crystalline form across all analyzed samples. A comparison of the shapes and intensities of the characteristic anatase peaks in the various XRD spectra reveals that the irradiation treatments of TiO_2 and its compositing with CNTs resulted in alterations to the structure and size of the nanoparticles. Notably, the as-prepared sample exhibited the most intense and distinct peaks, whereas the irradiated and composite samples displayed broader and less defined peaks. These findings imply that the as-prepared sample likely contained the largest nanoparticles and that the irradiation treatments and compositing led to a

reduction in nanoparticle size. Table 1 summarizes the crystal parameters determined through XRD and Raman measurements. Following exposure to ionizing radiation or the incorporation of CNTs, both the distance between atomic planes and the cell parameters increase, while the size of the particles diminishes due to electronic excitation or collective electron excitation. This effect is particularly pronounced when using SWCNTs, with TiO_2 nanoparticles decreasing in size from 16 nm to as low as 10 nm. The increase of the interplanar distance and cell parameters indicate an expansion of the crystal lattice which is the result of interaction of the TiO_2 crystalline lattice with both ionizing irradiation and CNTs.

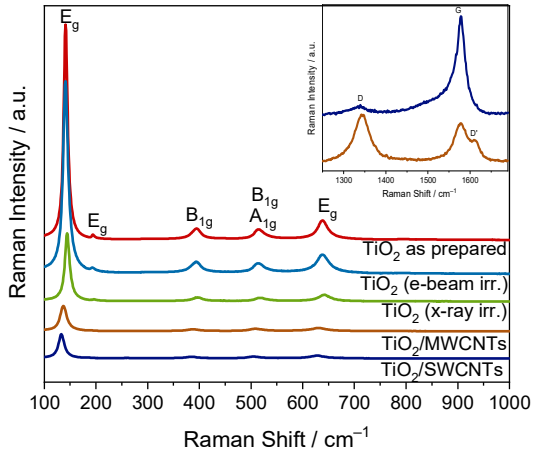

Figure 4 *Raman spectra of the studied samples*

The structural analysis conducted using Raman spectroscopy is illustrated in Fig. 4. The Raman modes observed in the spectra correspond to those of the anatase single crystal identified by Osaka [21]. The Raman spectra of the analyzed samples exhibit similar trends to those recorded by X-ray diffraction (XRD) analysis. For the irradiated samples or those composited with CNTs, the spectral features are less intense and broader compared to those of the as-prepared TiO_2.

The most intense Raman mode, E_g, displays a blue shift, meaning it shifts to higher wave number values as a result of irradiation (see Table 1). The shift and broadening of the Raman bands can be attributed to phonon confinement [22]. When irradiated, phonons become confined within the particles, leading to a decrease in particle size and an increase in the distribution of phonon momentum. Consequently, this results in the broadening of the Raman bands. Additionally, the presence of defects, such as oxygen vacancies, within the material can also influence the shift and broadening of the Raman bands [23]. Therefore, ionizing irradiation has a similar effect on oxygen vacancies as introducing certain

elements through doping [24]. Considering the phonon confinement model and the observed reduction in nanoparticle size due to the integration of CNTs, as indicated by the XRD analysis, it was initially anticipated that the prominent E_g vibrational modes would shift to higher wavenumbers (a blue shift) [25]. However, this expectation mainly applies to the pure TiO_2 system. In the case of the TiO_2/CNTs nanocomposites, a red shift was observed instead (shifts to higher wave number values). This red shift can be attributed to the strong interaction between TiO_2 and CNTs, which results in the formation of Ti-O-C bonds. Such bonding distorts the TiO_2 structure [26,27]. Furthermore, if the frequency of the phonons interacting with the incident photons decreases, the material experiences tensile strain, leading to an expansion of the crystalline lattice. Consequently, this results in a red shift of the Raman vibrational modes, which aligns well with the observations from the XRD analysis.

For the TiO_2 nanocomposites containing CNTs, several significant bands were detected in the Raman spectra region corresponding to CNTs, as shown in the intersect of Fig. 4. These include the D band, indicating the presence of disordered carbon; the G band, representing highly ordered carbon; and the D' bands associated with multi-walled carbon nanotubes (MWCNTs). Notably, these bands were shifted to higher wavenumbers than pure MWCNTs and single-walled carbon nanotubes (SWCNTs). This upshift indicates a strong interaction between TiO_2 and CNTs, which enhances charge transfer from TiO_2 to the CNTs.

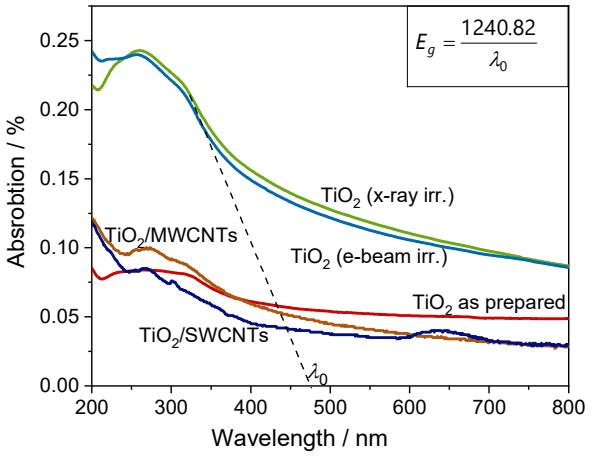

Figure 5 *UV-Vis spectra of the studied samples*

In Fig. 5, UV-Vis spectra of the sol-gel prepared TiO_2 before and after ionizing irradiations and compositing are shown. The cut-off wavelength (λ_0) is determined at the point where the tangent extended from the right side of the absorption peak intersects with the x-axis. The energy of the band gap (E_g) can be

calculated using the equation shown in the intersection of Fig. 5. The determined values of λ_0 and E_g are summarized in Table 2.

Table 2 *Calculated values of cut-off wavelength and energy of the band gap of the studied samples*

Sample	λ_0, nm	E_g, eV
as-prepared	427.58	2.90
e-beam irradiated	512.22	2.42
x-ray irradiated	523.07	2.37
TiO_2/MWCNTs	495.05	2.51
TiO_2/SWCNTs	521.02	2.38

In Figure 5, the UV-Vis spectra of sol-gel synthesized TiO_2, both prior to and after ionizing irradiation and compositing, are presented. The cut-off wavelength (λ) is identified at the intersection point where the tangent, drawn from the right side of the absorption peak, meets the x-axis. The energy of the band gap (E_g) is calculated using the equation indicated in the intersection of Figure 5. A summary of the values for λ_0 and E_g is provided in Table 2.

It is notable that the as-prepared TiO_2 nanoparticles display a significantly reduced band gap energy of 2.9 eV, in contrast to the 3.2 eV band gap energy of bulk anatase. This reduction suggests that structural modifications in TiO_2 resulting from ionizing irradiation contribute to a decrease in band gap energy. Specifically, the band gap energy diminishes from 2.9 eV to 2.42 eV with e-beam irradiation and to 2.37 eV with x-ray irradiation. Among the TiO_2/CNTs nanocomposites, the most pronounced reduction in band gap energy was observed in the composite containing single-walled carbon nanotubes (SWCNTs), where E_g decreased from 2.9 eV to 2.38 eV.

The results of this study, particularly concerning the effects of ionizing irradiation and the development of TiO_2 nanocomposite materials using carbon nanotubes (CNTs), represent a noteworthy advancement in the field. They highlight a significant achievement in reducing the band gap energy of TiO_2 in comparison to existing literature [6-14].

CONCLUSIONS

The research findings indicate that both ionizing radiations, such as X-rays and electron beams, as well as the incorporation of carbon nanotubes (CNTs), result in similar structural changes in titanium dioxide (TiO2). These changes encompass a decrease in nanoparticle size, an increase in interplanar distance, and alterations to lattice parameters. Consequently, these structural modifications lead

to a reduction in band gap energy, which shifts light absorption into the visible spectrum and enhances photocatalytic activity.

Acknowledgments: This paper has been supported by the Science and Research Fund of Ss. Cyril and Methodius University in Skopje, 2024.

REFERENCES

1. P. Thangadurai, R. Beura, J. S. Kumar, *Nanomaterials with Different Morphologies for Photocatalysis*, in *Green Photocatalysts*, M. Naushad, S. Rajendran, E Lichtfouse, Eds., Springer Nature, Switzerland, 2000, p. 47-87. https://doi.org/10.1007/978-3-030-15608-4_3

2. S. Peiris, Haritha, B. de Silva, K. N. Ranasinghe, I. R. Perera, Recent development and future prospects of TiO_2 photocatalysis, *Journal of the Chinese Chemical Society* **68** (2021) 739–769. https://doi.org/10.1002/jccs.202000465

3. M. B. Tahir, M. Sohaib, M. Sagir, M. Rafique, Role of nanotechnology in photocatalysis, *Encyclopedia of Smart Materials* **2** (2022) 578-589. https://doi.org/10.1016/B978-0-12-815732-9.00006-1

4. A. Fujishima, K. Honda, Electrochemical photolysis of water at a semiconductor electrode, *Nature* **238** (1972) 37-38. https://doi.org/10.1038/238037a0

5. T. Luttrell, S. Halpegamage, J. Tao, A. Kramer, E. Sutter, M. Batzill, Why is anatase a better photocatalyst than rutile? - Model studies on epitaxial TiO_2 films, *Scientific Reports* **4** (2014) 4043. https://doi.org/10.1038/srep04043

6. A. Zaleska, Doped-TiO_2: A Review, *Recent Patents on Engineering* **2** (2008) 157-164. https://doi.org/10.2174/187221208786306289

7. M. B. Kanoun, F. Ahmed, C. Awada, C. Jonin, P-F. Brevet, Band gap engineering of Au doping and Au – N codoping into anatase TiO_2 for enhancing the visible light photocatalytic performance, *International Journal of Hydrogen Energy* **51** (2024) 907-913. https://doi.org/10.1016/j.ijhydene.2023.10.244

8. M. Toyoda, T. Yano, B. Tryba, S. Mozia, T. Tsumura, M. Inagaki, Preparation of carbon-coated Magneli phases Ti_nO_{2n-1} and their photocatalytic activity under visible light, *Applied Catalysis B: Environment* **88** (2008) 160-164. https://doi.org/10.1016/j.apcatb.2008.09.009

9. H. An, S. Y. Park, H. Kim, C. Y. Lee, S. Choi, S. C. Lee, S. Seo, E. C. Park, Y. Oh, C. Song, J. Won, Y. J. Kim, J. Lee, H. U. Lee, Y. Lee, Advanced nanoporous TiO_2 photocatalysts by hydrogen plasma for efficient solar-light photocatalytic application, *Scientific Reports* 6 (2016) 29683. https://doi.org/10.1038/srep29683

10. K.P. Priyanka, S. Joseph, A.T. Sunny, T. Varghese, Effect of high energy electron beam irradiation on the optical properties of nanocrystalline TiO_2, *Nanosystems: Physics, Chemistry, Mathematics* **4** (2013) 218-224.

11. M.C. Molina Higgins, J.V. Rojas, X-ray radiation enhancement of gold-TiO_2 nanocomposites, *Applied Surface Science* **480** (2019) 1147-1155. https://doi.org/10.1016/j.apsusc.2019.02.234

12. K.R. Diab, M.M. Doheim, S.A. Mahmoud, S.A. Shama, H.A. El-Boohy, Gamma-Irradiation Improves the Photocatalytic Activity of Fe/TiO_2 for Photocatalytic Degradation of 2-Chlorophenol, *Chemistry and Materials Research* **9** (2017) 49-60.
13. W.D. Wang, P. Serp, P. Kalck, J.L. Faria, Visible light photodegradation of phenol on MWNT-TiO_2 composite catalysts prepared by a modified sol–gel method, *Journal of Molecular Catalysis A: Chemical* **235** (2005) 194. https://doi.org/10.1016/j.molcata.2005.02.027
14. P. Paunović, A. Grozdanov, P. Makreski, I. Dimitrievska, A. Petrovski, Structural changes of TiO_2 as a result of CNTs incorporation, *Material Science & Engineering International Journal* **6** (2022) 31-39. https://doi.org/10.15406/mseij.2022.06.00177
15. P. Paunović, A. Grozdanov, P. Makreski, G. Gentile, A.T. Dimitrov, *Application of Ionizing Irradiation for Structure Modification of Nanomaterials*, in *Nanoscience and Nanotechnology in Security and Protection against CBRN Threats*, P. Petkov, M.E. Achour, C. Popov, Eds., Springer Nature B.V., Dordrecht, The Netherlands, 2020, p. 23-43. https://doi.org/10.1007/978-94-024-2018-0_2
16. S.S. Latthe, S. An, S. Jin, S.S. Yoon, High energy electron beam irradiated TiO_2 photoanodes for improved water splitting, *Journal of Materials Chemistry A* **1** (2013) 13567-13575. https://doi.org/10.1039/C3TA13481D
17. P. Wronski, J. Surmacki, H. Abramczyk, A. Adamus, M. Nowosielska, W. Maniukiewicz, M. Kozanecki, M. Szadkowska-Nicze, Surface, optical and photocatalytic properties of silica-supported TiO_2 treated with electron beam, *Radiation Physics and Chemistry* **109** (2015) 40-47. https://doi.org/10.1016/j.radphyschem.2014.12.009
18. S.S. Surah, M. Vishwakarma, R. Kumar, R. Nain, S. Sirohi, G. Kumar, Tuning the electronic band alignment properties of TiO_2 nanotubes by boron doping, *Results in Physics* **12** (2019) 1725-1731. https://doi.org/10.1016/j.rinp.2019.01.081
19. Z. Dong, W. Li, H. Wang, X. Jiang, H. Liu, L. Zhu, H. Chen, Carbon nanotubes in perovskite-based optoelectronic devices, *Matter* **5** (2022) 448-481. https://doi.org/10.1016/j.matt.2021.12.011
20. M. Shaban, A.M. Ashraf, M.R. Abukhadra, TiO_2 nanoribbons/carbon nanotubes composite with enhanced photocatalytic activity; fabrication, characterization, and application, *Scientific Reports* **8** (2017) 781. https://doi.org/10.1038/s41598-018-19172-w
21. T. Oshaka, F. Izumi, Y. Fujiki, Raman spectrum of anatase TiO_2, *Journal of Raman Spectroscopy* **7** (1978) 321-324. https://doi.org/10.1002/jrs.1250070606
22. H.C. Choi, Y.M. Jung, S.B. Kim, Size effects in the Raman spectra of TiO_2 nanoparticles *Vibrational Spectroscopy* **37** (2005) 33-38. https://doi.org/10.1016/j.vibspec.2004.05.006
[23. J.C. Parker, R.W. Siegel, Raman microprobe study of nanophase TiO_2 and oxidation-induced spectral changes, *Journal of Materials Research* **5** (1990) 1246-1252. https://doi.org/10.1557/JMR.1990.1246
24. M.M. Khan, S.A. Ansari, D. Pradhan, M.O. Ansari, D.H. Han, J. Lee, M.H. Cho, Band gap engineered TiO_2 nanoparticles for visible light induced photoelectrochemical and photocatalytic studies, *Journal of Materials Chemistry A* **2** (2014) 637-644. https://doi.org/10.1039/C3TA14052K
25. C.Y. Xu, P.X. Zhang, L. Yan, Blue shift of Raman peak from coated TiO_2 nanoparticles, *Journal of Raman Spectroscopy* **32** (2001) 862-865. https://doi.org/10.1002/jrs.773

26. M.M. Gui, S-P. Chai, B-Q. Xu, A.R. Mohamed, Visible-light-driven MWCNT@TiO_2 core–shell nanocomposites and the roles of MWCNTs on the surface chemistry, optical properties and reactivity in CO_2 photoreduction, *RSC Advances* **4** (2014) 24007-24013. https://doi.org/10.1039/C4RA02561J
27. A. Saha, A. Moya, A. Kahnt, D. Iglesias, S. Marchesan, R. Wannemacher, M. Prato, J.J. Vilatela, D.M. Guldi, Interfacial charge transfer in functionalized multi-walled carbon nanotube@TiO_2 nanofibres, *Nanoscale* **9** (2017) 7911-7921. https://doi.org/10.1039/C7NR00759K